[3]Browning, C. E., Husman, G. E., and Whitney, J. M., "Moisture Effects in Epoxy Matrix Composites," *Composite Materials: Testing and Design (Fourth Conference)*, STP 617, American Society for Testing and Materials, Philadelphia, 1977, pp. 481-496.

[4]Pipes, R. B., Vinson, J. R., and Tsu-Wei, C., "On the Hygrothermal Response of Laminated Systems," *Journal of Composite Materials,* Vol. 10, April, 1976, pp. 129-148.

[5]Chi-Hung, S., and Springer, G. S., "Environmental Effects on the Elastic Moduli of Composite Materials," *Journal of Composite Materials,* Vol. 11, July 1977, pp. 250-264.

[6]Crank, J., *The Mathematics of Diffusion* (2nd ed.), Clarendon Press, Oxford, England, 1975.

[7]Snead, J. M., and Palazotto, A. N., "Moisture and Temperature Effects on the Instability of Cylindrical Composite Panels," *Journal of Aircraft,* Vol. 20, Sept. 1983, pp. 777-783.

[8]Straw, A. D. and Palazotto, A. N., "The Shear Buckling of Composite Cylindrical Panels Considering Environmental Effects," AIAA Paper 86-0879, 1986.

[9]Almroth, B. O. and Brogan, F. A., *Users Manual for STAGS, Vol. 1, Theory,* Structural Mechanics Laboratory, Lockheed Palo Alto Research Laboratory, Palo Alto, CA, March 1978.

[10]Straw. A. D., "The Buckling of Composite Cylindrical Panels Considering Environmental Effects," M.S. Thesis, Air Force Institute of Technology, Wright-Patterson AFB, OH, Dec. 1985.

Full-Potential Circular Wake Solution of a Twisted Rotor Blade in Hover

Hans R. Aggarwal*
Helicopter Aerodynamics and Noise
Mountain View, California

Introduction

An exact solution to the flow past a rotor blade is quite difficult because of the nonuniform, complicated flow in its vicinity. A few approximate solutions, employing both transonic small disturbance and full-potential aerodynamic theories with prescribed wakes, have been obtained in the past.[1-5] This Note uses a modified version of the full-potential code ROT22 and presents, employing a simple, circular wake, a solution for the transonic flow past a twisted rotor blade in hover. The flow is also evaluated for a fixed-wing-type straight wake, previously used in Ref. 1, and the results of the two calculations are compared. The results of the circular wake solution are also compared with those for a cambered section obtained on the basis of a general two-dimensional wake.[5] It is shown that the circular wake and the general two-dimensional wake solutions have similar characteristics.

Flow Equations and ROT22

Consider a helicopter hovering with a rotational speed ω. Let $O(x,y,z)$ be a (clockwise) orthogonal blade-fixed Cartesian coordinate system with the z axis running along the blade span and the x axis running parallel to a blade-section chord pointing towards the trailing edge. For a full-potential (nonconservative, irrotational, isentropic) quasisteady flow, the equations governing the flow in the blade-fixed (rotating) coordinate system, reduce to

$$(a^2-q_1^2)\phi_{xx}+(a^2-q_2^2)\phi_{yy}+(a^2-q_3^2)\phi_{zz}-2q_1q_2\phi_{xy}$$
$$-2q_2q_3\phi_{yz}-2q_3q_1\phi_{zx}+\omega^2(x\phi_x+z\phi_z)=0 \tag{1}$$

and the Bernoulli equation

$$\omega(z\phi_x-x\phi_z)+\tfrac{1}{2}(\phi_x^2+\phi_y^2+\phi_z^2)+[a^2/(\gamma-1)]=\text{const} \tag{2}$$

where a is the local speed of sound, ϕ the full-velocity potential, q_i, $(i=1,2,3)$, the x,y,z components of the local velocity vector q defined by

$$q_1=\phi_x+\omega z \qquad q_2=\phi_y \qquad q_3=\phi_z-\omega x \tag{3}$$

γ is the ratio of specific heats. Equation (2) relates the local speed of sound to the velocity potential. The equations are quasisteady in the sense that the time derivatives in the flow equations are ignored. To complete the formulation of the problem, several boundary conditions are necessary. On the blade surface, the flow is tangential and, therefore, requires that $q\cdot\nabla F(x,y,z)=0$, where $F(x,y,z)=0$ is the equation of the blade surface. To satisfy the Kutta condition, an inviscid wake, taken as a vortex sheet, is assumed to lie on a surface continued smoothly behind the trailing edge of the rotor. It is also assumed that the jump in velocity potential along the circular trajectory, traced by a given point on the trailing edge, remains constant during the flow; and the velocity-potential gradient vanishes at large distances from the rotor.

The code ROT22, originally adapted from Jameson's fixed-wing code FLO22,[6] was modified to allow for the variable twist of the rotor blade. The implementation of the circular wake requires locating the point on the trailing edge that last passed through a given point of the wake. If (r,θ) are the polar coordinates of a point P in the wake, referred to in the current position of the leading edge as the initial line, and (x_0,z_0) the Cartesian coordinates of the point P_0 on the trailing edge that was at P at some earlier time t, then the two sets of coordinates are related by the equations

$$x_0=r\sin(\theta+\omega t) \qquad z_0=r\cos(\theta+\omega t) \tag{4}$$

Equations (4), together with the equation of the trailing edge, uniquely determine the coordinates (x_0,z_0) in any given revolution of the blade. This root finding is achieved through a newly developed subroutine C wake. It may be remarked in passing that the subroutine C wake may be extended without any difficulty to noncircular trajectories corresponding to an advancing helicopter. The solution for a given tip Mach number (TMN) on any mesh is obtained iteratively until the maximum correction in the velocity potential is reduced to less than $1.0E-5$.

The model example considered is that of a 1/7th scale UH−1H NACA 0012 profile, single, straight, rotor with input parameters taken as blade outer radius, $R_0=1.045$ m; blade inner radius, $R_i=0.151$ m; and blade chord, $c=0.0762$ m. The twist along the rotor was assumed linear and given by the equation

$$\alpha=10(1-z/R_0) \tag{5}$$

prescribing a washout of 10 deg at the blade root. The fluid density ρ_0 of the undisturbed medium, assumed at 60°F, was taken as 1.225 kg/m.

Results and Discussion

Figure 1 exhibits the distribution of the local lift coefficient C_L defined by

$$C_L=\frac{2}{\rho_0\omega^2z^2c}\int(p_\ell-p_u)\mathrm{d}x \tag{6}$$

for TMN = 0.9 along the blade span, as predicted by the circular and straight wakes. In Eq. (6), p_ℓ and p_u are the lower and upper surface pressures, respectively, at span station z. Figure 1 shows that the effect of the curvature of the wake is

Received April 10, 1986.

*Senior Research Associate.

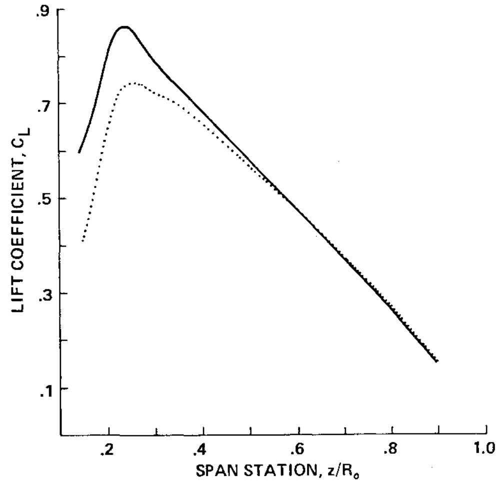

Fig. 1 Local lift coefficient as a function of blade span coordinate z/R_0. TMN = 0.9; —, C wake; ...., straight wake.

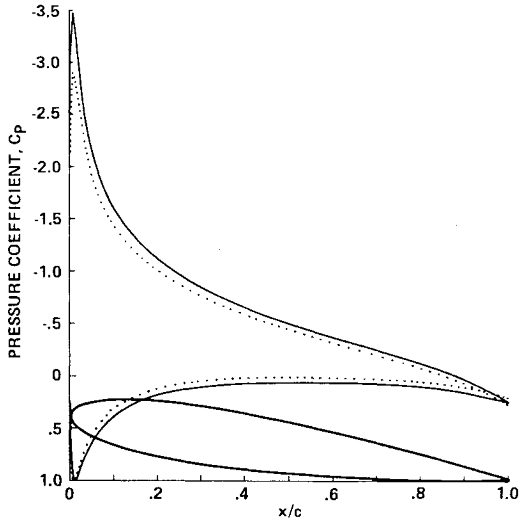

Fig. 2 Pressure coefficient at $z/R_0 = 0.235$, as a function of section chordwise coordinate x/c. TMN = 0.9; —, C wake; ...., straight wake.

maximum at a station near the inboard tip. This was expected since the curvature of the circular trajectories decreases with increasing distance along the blade span. It is also seen that the straight wake tends to slightly overpredict the lift coefficients toward the outer blade stations. The maximum difference between the results in Fig. 1 may be smaller if the lift coefficient were calculated using the dynamic pressure based on tip speed instead of local speeds. This would be misrepresenting the results since it is the local lift coefficient that is usually referred to in literature.[7] Figure 2 shows the distribution of the pressure coefficient C_p defined by

$$C_p = [2/(\rho_0 \omega^2 z^2)]\,(p - p_0) \tag{7}$$

as a function of the chordwise coordinate x/c at an inner blade span station $z/R_0 = 0.235$, where the lift coefficient is close to its peak value. (The tilt of the blade profile at the bottom of the figure is due to the washout angle at the span station under consideration.) One notes that upper and lower pressure distribution curves for the straight wake do not match well near the trailing edge, whereas the pressures for the circular wake modification match exactly. This situation may imply that the circular wake modification better satisfies the Kutta condition. It may, alternatively, be compared to a starting vortex since a straight wake suddenly is being imposed on inboard blade sections, which are moving in relatively highly curved circular paths.

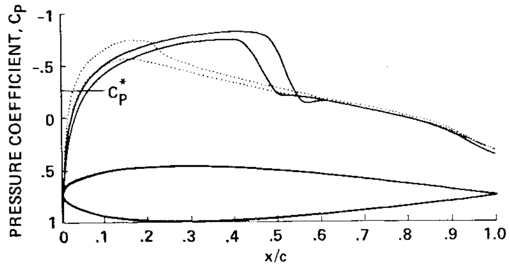

Fig. 3 Pressure coefficient at $z/R_0 = 1.006$, C wake case, as a function of section chordwise x/c. —, TMN = 0.9; ...., TMN = 0.8.

The circular wake modification observations are consistent with the observations made by Chang and Tung,[5] who considered a cambered section and used the Bernoulli equation to compute the jumps in the velocity potential at points in the wake, and assumed a planar wake behind the trailing edge. The circular wake is relatively simpler to use since it avoids solving the Bernoulli equation each time, at each computational point of the wake. The accuracy of a lift distribution curve computed on the basis of a two-dimensional wake, like the one in Fig. 1 or Fig. 4 in Ref. 5, is, of course, limited. It should be recalled that a two-dimensional wake ignores the roll up of the wake and also neglects the effect of the induced velocity and the tip vortex on the computation. Another factor affecting the accuracy is that a computation based on FLO22 and ROT22 codes can only make use of the near wake. The latter point is specifically made in Ref. 4.

Figure 3 shows the distribution of the pressure coefficient C for TMN's 0.8 and 0.9 as a function of the chordwise coordinate x/c at span station $z/R = 1.006$. Computation of the pressure coefficient for other TMN's shows that the influence of the tip Mach number increases with the distance along the blade. Comparing the solid-line curves in Figs. 2 and 3, note how the spiky behavior of the pressure distribution curves observed near the inboard blade stations get smoother at the outer blade stations but apparently culminate in a shock wave.

Acknowledgments

This work was carried out under NASA Ames Research Center Contract NAS2-12072 with Helicopter Aerodynamics and Noise. The author thanks Dr. Sanford Davis for his support.

References

[1]Arieli, R. and Tauber, M.E., "Computation of Subsonic and Transonic Flow About Lifting Rotor Blades," AIAA Paper 79-1667, Atmospheric Flight Mechanics Conference, Boulder, CO, Aug. 6–8, 1979.

[2]Caradonna, F.X., Tung, C., and Desopper, A., "Finite Difference Modeling of Rotor Flows Including Wake Effects," paper presented at the Eighth European Rotorcraft Forum, Aix-en-Provence, France, Aug. 31–Sept. 3, 1982.

[3]Tung, C., Caradonna, F.X., Boxwell, D.A., and Johnson, W.R., "The Prediction of Transonic Flows on Advancing Rotors," Paper 84-40-44-1, presented at the 40th Annual National Forum of the American Helicopter Society, Arlington, VA, May 16–18, 1984.

[4]Egolf, T.A. and Sparks, S.P., "Hovering Rotor Airload Prediction Using a Full-Potential Flow Analysis with Realistic Wake Geometry," paper presented at the 41st Annual National Forum of the American Helicopter Society, Ft. Worth, TX, May 15–17, 1985.

[5]Chang, I.C. and Tung, C., "Numerical Solution of the Full-Potential Equation for Rotors and Oblique Wings using a New Wake Model," AIAA Paper 85-0268, 1985.

[6]Jameson, A. and Caughey, D.A., "Numerical Calculation of the Transonic Flow Past a Swept Wing," Courant Institute of Mathematical Sciences, COO-3077-140, June 1977.

[7]Stepniewski, W.Z., "Rotary-Wing Aerodynamics," *Basic Theories of Rotor Aerodynamics (With Application to Helicopters)*, Vol. 1, NASA CR 3082 1979, p. 286.